1 **The Thr300Ala variant of ATG16L1 is associated with decreased risk of brain**
2 **metastasis in patients with non-small cell lung cancer**

3 Qian-xia Li,[1] Xiao Zhou,[1] Ting-ting Huang,[1] Yang Tang,[1] Bo Liu,[1] Ping Peng,[1] Li
4 Sun,[1] Yi-hua Wang,[2] and Xiang-lin Yuan[1*]
5 [1]Department of Oncology, Tongji Hospital, Huazhong University of Science and
6 Technology, Wuhan, Hubei Province, China; and [2]Centre for Biological Sciences, The
7 University of Southampton, Southampton, SO17 1BJ , United Kingdom

8 **Keywords:** autophagy, brain metastasis, non-small cell lung cancer, SNPs, ATG16L1,
9 prevention

10 **Abbreviations:** BM, brain metastases; CDH2, cadherin 2; CI, confidence interval;
11 DFS, disease-free survival; EMT, Epithelial-to-mesenchymal transition; NSCLC,
12 non-small cell lung cancer; KPS, Karnofsky performance status; HR, hazard ratios;
13 QoL, quality of life; SNPs, single nucleotide polymorphisms; PCI, prophylactic
14 cranial irradiation.

15 **Corresponding author**: Xiang-lin Yuan, Department of Oncology, Tongji Hospital,
16 Huazhong University of Science and Technology, Wuhan, Hubei Province, China;
17 e-mail yxl@medmail.com.cn

18 **Abstract**

19 Non-small cell lung cancer (NSCLC) often metastasizes to the brain, but
20 identifying which patients will develop brain metastases (BM) is difficult. Autophagy
21 is critical for cancer initiation and progression. We hypothesized that genetic variants
22 of autophagy-related genes may affect brain metastases (BM) in NSCLC patients. We
23 genotyped 16 single nucleotide polymorphisms (SNPs) in seven autophagy-related
24 genes (*ATG3*, *ATG5*, *ATG7*, *ATG10*, *ATG12*, *ATG16L1*, and *LC3*) by using DNA from
25 blood samples of 323 NSCLC patients. Further, we evaluated the potential

associations of these genes with subsequent BM development. Lung cancer cell lines stably transfected with *ATG16L1*: rs2241880 (T300A) were established. Mouse models of brain metastasis were developed using cells transfected with *ATG16L1*-300T or *ATG16L1*-300A. *ATG10*: rs10036653 and *ATG16L1*: rs2241880 were significantly associated with a decreased risk of BM (respective hazard ratios [HRs] = 0.596, 95% confidence interval [CI] 0.398–0.894, *P* = 0.012; and HR =0. 655, 95% CI 0.438–0.978, *P* = 0.039, respectively]. *ATG12*: rs26532 was significantly associated with an increased risk of BM (HR = 1.644, 95% CI 1.049–2.576, *P* = 0.030]. Invasion and migration assays indicated that transfection with *ATG16L1*-300T (vs. 300A) stimulated the migration of A549 cells. An *in-vivo* metastasis assay revealed that transfection with *ATG16L1*-300T (vs. 300A) significantly increased brain metastasis. Our results indicate that genetic variations in autophagy-related genes can predict BM and that genome analysis would facilitate stratification of patients for BM prevention trials.

Introduction

More than 1,50,000 patients with cancer are diagnosed with brain metastasis every year, [1] with the lung being the most common primary site for secondary BM. [2,3] Brain metastases (BM) in patients with non-small cell lung cancer (NSCLC) are a devastating problem with profound impact on survival and quality of life (QoL). Survival times after BM diagnosis remain poor at only 1.5–9.5 months. [4,5] Although studies have shown that prophylactic cranial irradiation (PCI) is successful in decreasing the incidence of BM, [6-9] preventive treatments for BM are rarely employed in clinical practice because of the lack of proven survival advantage and the potential for toxicity. This negative result on survival may be explained by the unintended selection of patients with a low risk of cerebral metastasis. A recent trial revealed that

51 PCI provides significantly lengthened disease-free survival (DFS), but does not have a
52 significant effect on overall survival (OS). In this study, all patients who received PCI
53 were selected on the basis of risk factors of brain metastases; however, these risk
54 factors have not been clarified. [10] These findings suggest that PCI may not be suitable
55 for all patients. Therefore, it is necessary to identify the population subset that is at the
56 highest risk of BM and is most likely to benefit from PCI.

57 Pretreatment factors that predict high rates of BM include histology, extent of
58 disease, and young age. However, previously published studies have reported
59 conflicting results. [11-13] Furthermore, these studies did not consider genetic factors.
60 Only one study has reported that the expression levels of three genes, *CDH2*, *KIFC1*,
61 and *FALZ*, are highly predictive of BM in early and advanced lung cancer. [14] The
62 expression levels of genes are affected by several factors; this limits the applicability
63 of the genomic approach for risk prediction. Improvements in predictive accuracy
64 require the identification and inclusion of molecular markers of the risk of BM.

65 One approach to identifying molecular markers involves studying single nucleotide
66 polymorphisms (SNPs) in signaling pathways that regulate cell proliferation and
67 migration, and assessing the relationship between multiple SNPs and the risk of BM.
68 We previously reported that genetic variations in the PtdIns3P-AKT pathway are
69 associated with an increased risk of BM in patients with NSCLC. [15] Additional
70 investigations on candidate genes that are crucial for metastasis may uncover missing
71 links in the heritability of BM. Autophagy is an important adaptive prosurvival
72 mechanism that mediates cancer cell survival during metastasis. In this study, we
73 expand on our previous results by analyzing SNPs in the autophagy pathway.

74 Autophagy is a lysosomal degradation process that regulates of the turnover of
75 damaged proteins and organelles and promotes cell survival during nutrient

76 deprivation or micro-environmental stress. [16] Cancer cells face diverse environmental
77 and cellular stresses during metastatic progression. [17] To cope with this, tumor cells
78 induce adaptive pathways such as autophagy. [18,19] A previous study has reported that
79 autophagy inhibition suppresses pulmonary metastasis of hepatocellular carcinoma in
80 mice. [20] Another study revealed that upregulated autophagy further enhances
81 epithelial-to-mesenchymal transition (EMT) and migration ability in pancreatic cell
82 lines. [21] EMT is a reversible phenotypic change in which cells lose intercellular
83 adhesion and epithelial polarization, and gain motility and invasiveness. [22] In cancer,
84 EMT has been shown to play a key role in the induction of cancer cell invasion and
85 metastasis. [23]

86 During the formation of mammalian autophagosomes, two ubiquitin-like protein
87 conjugation systems, Atg12-conjugation and LC3-modification, are required, and
88 autophagy related genes (*ATG3*, *ATG5*, *ATG7*, *ATG10*, *ATG12*, *ATG16L1*, and *LC3*)
89 are involved in this process. Increased ATG10 expression was observed in colorectal
90 cancer associated with lymphovascular invasion and lymph node metastasis. [24]
91 Recently, Desai et al. revealed that high ATG7 expression level was associated with
92 poor patient survival in breast cancer. [25] Similar important roles of ATGs have also
93 been demonstrated in the development of other cancers. [26,27] Together, these findings
94 indicate that autophagy plays an important role in carcinogenesis. To our knowledge,
95 no study has focused on the association between polymorphisms in the *ATG* genes
96 and the risk of BM in patients with NSCLC. Therefore, we sought to identify potential
97 associations between genetic variations in seven genes in this pathway—*ATG3*, *ATG5*,
98 *ATG7*, *ATG10*, *ATG12*, *ATG16L1*, and *LC3*—with the occurrence of BM in patients
99 with NSCLC to identify potential candidates for intervention to reduce brain relapses.

100 Results

101 **Patient characteristics**

102 The characteristics of the 323 patients (221 men and 102 women) included in the
103 study are listed in Table 1. At a median follow-up interval of 25 months (range, 0–135
104 months), BM had developed in 101 patients. The following sites of metastases were
105 noted: brain only (n = 31); bone, lungs, adrenals, liver, and other unspecified sites (n =
106 148), or both (n = 70). Of the 70 patients who had metastases in both the brain and
107 other sites, 10 had BM as the first site of recurrence, 45 had first recurrence at other
108 sites, and 15 had simultaneous recurrence in more than one site. The median age of all
109 patients was 57 years (range, 26–82 years); 54% had stage I-IIIA disease; 69% had
110 adenocarcinoma, and 51% had smoked tobacco (72.4% of men and 5.9% of women).
111 The median time from NSCLC diagnosis to the detection of BM was 9 months.
112 Univariate and multivariate analyses (Table 1) of patient- and tumor-related
113 characteristics and BM revealed that disease stage was associated with BM, with
114 patients having stage IIIB or stage IV disease at a higher risk of BM ($P < 0.001$).
115 Neither tumor histology nor smoking status was associated with BM in this
116 population.

117 **Effects of single SNPs on the risk of BM**

118 We assessed the potential association of each of the 16 individual SNPs with BM
119 risk by using a multivariate Cox model. We found that three SNPs, *ATG10*:
120 rs10036653, *ATG16L1*: rs2241880, and *ATG12*: rs26532 were associated with BM
121 risk. BM rates were lower for patients with the AT/TT genotype of *ATG10*:
122 rs10036653 ($P = 0.063$, Figure 1A) and the AG/GG genotype of *ATG16L1*: rs2241880
123 ($P = 0.014$, Figure 1B). BM rates were higher for patients with the AC/CC genotype
124 of *ATG12*: rs26532 ($P = 0.015$, Figure 1C). In general, BM developed less often in
125 patients with the AT/TT genotype of *ATG10*: rs10036653 (39%), the AG/GG genotype

126 of *ATG16L1*: rs2241880 (39%), or the AA genotype of *ATG12*: rs26532 (37%) than in
127 patients with the AA (29%), AA (26%), or AC/CC genotypes (22%; Table 2).
128 Multivariate Cox proportional hazard analyses showed that the AT/TT genotype of
129 *ATG10*: rs10036653 and the AG/GG genotype of *ATG16L1*: rs2241880 are associated
130 with a significantly lower risk of BM (hazard ratio [HR] 0.596, 95% confidence
131 interval [CI] 0.398–0.894, $P = 0.012$; and HR 0.655, 95% CI 0.438–0.978, $P = 0.039$,
132 respectively), and that the AA genotype of *ATG12*: rs26532 is associated with a
133 significantly higher risk of BM (HR 1.644, 95% CI 1.049–2.576, $P = 0.030$), after
134 adjustment for gender, patient age, disease stage, tumor histology, Karnofsky
135 performance status (KPS), and smoking status. However, the *ATG10* genotype was
136 significant only in the multivariate analysis. Similar analyses of the other 13 SNPs
137 showed no associations between any other genotype and the incidence of BM
138 (Supplementary Table). None of the three genotypes tested was associated with
139 metastasis at sites other than the brain (data not shown).

140 **Combined effect of SNPs on the risk of BM**

141 To analyze the combined effect of SNPs on the risk of BM, we defined the AA
142 genotype of *ATG16L1*: rs2241880 and the AC/CC genotypes of *ATG12*: rs26532,
143 which are associated with an increased risk of BM, as “unfavorable” genotypes. When
144 we grouped the patients according to the number of unfavorable genotypes (i.e., 0, 1,
145 or 2), the risk of BM increased with as the number of unfavorable genotypes
146 increased; BM developed in 45% of patients with both unfavorable genotypes, in 31%
147 of those with either unfavorable genotype, and in 17% of those with no unfavorable
148 genotype. This increase in the risk of developing BM from having both unfavorable
149 genotypes was confirmed by Kaplan–Meier analyses ($P = 0.002$, Figure 1D).
150 Multivariate Cox proportional hazard analyses showed that the HR for individuals

with one unfavorable genotype was 1.942 (95% CI 1.010–3.735, *P* = 0.047), and the HR for those with both unfavorable genotypes was 3.051 (95% CI 1.543–6.033, *P* = 0.001; Table 3).

***ATG16L1*-300T increases cell migration and invasion**

We also tested if the *ATG16L1*: rs2241880 (T300A) variant genotype influenced the metastatic potential of lung cancer cells *in vitro*. First, two A549 cell lines stably transfected with *ATG16L1* (300T or 300A) were established via lentivirus-mediated transfection (Figure 2). The transfection efficiency for the A549 lung cancer cell lines was approximately 99%. Cell migration and cell invasiveness were assessed by using Transwell® assays. Upon transfection with the *ATG16L1*-300T construct, the cell line demonstrated increased motility relative to the 300A transfectants (Figure 3). These results suggest that the *ATG16L1*-300T genotype increased the metastatic potential of this lung cancer cell line.

***ATG16L1*-300T increases BM in nude mice**

To explore whether autophagy plays a role in brain metastasis, we examined the effect of the *ATG16L1*: rs2241880 (T300A) variant genotypes on A549 metastasis in a nude mouse model of brain metastasis. The model was established with A549-300T/A549-300A cells, and a control cell line (A549-Mock) was established with a control virus. Two mouse died one week after intracardiac injection with the A549-300T/A549-300A cells, and these two mouse were excluded from the study. In the A549-Mock group, one mouse died at the seventh week after intracardiac injection. However, histological examination confirmed that brain metastasis had not occurred in this mouse, and therefore, we included it in the final analysis. Consequently, there were eight mice in the A549-Mock group and seven mic e in the A549-300T/A549-300 group at the time of the final analysis in the 7th week.

Small-animal imaging analysis of the nude mouse model using green fluorescent protein (GFP)-luciferase-expressing A549-300T, A549-300A, and A549-Mock cells corroborated the results of the histopathological analysis (Figure 4). In summary, the percentage of BM in the A549-300T group (42.9%) was higher than that in the A549-300A group (14.2%) and the A549-Mock group (12.5%).

Discussion

In this study, we investigated whether genetic variations in the autophagy-related genes, *ATG3*, *ATG5*, *ATG7*, *ATG10*, *ATG12*, *ATG16L1*, and *LC3*, are associated with BM risk. We found that SNPs in *ATG10*: rs10036653, *ATG16L1*: rs2241880, or *ATG12*: rs26532 were associated with BM.

One of the polymorphisms associated with BM risk was in *ATG16L1*. This gene has been mapped to chromosome 2q37.1, [28] and the SNP in the *ATG16L1* c.898A>G (rs2241880) gene results in the substitution of threonine with alanine (T300A/Thr300Ala), thereby changing the polarity of the protein. This SNP has been shown to affect the autophagy process, [29] and the G allele has been identified as a risk allele in Crohn's disease. [30,31] One possible explanation for the observed association between the *ATG16L1* genotype and BM is that this effect is mediated through modulation of the pro-inflammatory cytokine interleukin IL1B. The T300A polymorphism significantly increases caspase 3- and caspase 7-mediated cleavage of ATG16L1, resulting in lower levels of full-length ATG16Ll T300A protein. [32] Loss of the autophagy protein ATG16L1 enhances endotoxin-induced IL1B production. [33] Besides its functional role in immune responses, IL1B also affects the cell growth and differentiation of various cell types.[34] Similar to our findings, the presence of the *ATG16L1* G allele has been associated with a protective effect against epithelial thyroid carcinoma. [27] In a recent study, *ATG16L1* (T300A) was found to be associated

201 with reduced metastasis in colorectal cancer patients. [35] Collectively, these
202 observations indicate that our finding of an association between SNPs and BM in
203 patients with NSCLC may be biologically plausible.

204 We also found that the *ATG10*: rs10036653 and *ATG12*: rs26532 polymorphisms
205 are associated with BM risk. ATG10, which is an autophagic E2 enzyme, interacts
206 with ATG7 to receive an ubiquitin-like molecule ATG12. Additionally, ATG10 and
207 ATG12 are involved in the ATG12–ATG5 conjugation reaction. [36] The chromosomal
208 region of ATG10 (5q24) is frequently lost in multiple cancers. [37,38] In a recent study,
209 SNPs in ATG10 were found to be associated with the risk of developing breast
210 cancer.[39] Increased ATG10 expression in colorectal cancer is associated with
211 lymphovascular invasion and lymph node metastasis, [24] suggesting that *ATG10* is an
212 oncogene. However, univariate analysis has indicated that the *ATG10* genotype is not
213 a significant prediction factor. Together, these data suggest that the *ATG10* variant
214 may be an independent predictor of the risk of developing BM, but interference by
215 other tumor characteristics cannot be excluded and needs to be studied in a
216 multifactorial model in future studies. Additionally, the biology of *AGT10* in the
217 development of lung cancer needs to be investigated further.

218 The complex nature of cellular signaling pathways often means that a single SNP
219 may produce only a modest or undetectable effect, whereas the amplified effects of
220 combined SNPs in the same pathway may enhance the predictive power of genome
221 analysis. When we combined two SNPs in two different genes, both showing
222 significant association with BM, we found substantial increases in the risk of BM for
223 patients with two unfavorable genotypes compared with those with no unfavorable
224 genotypes. These results suggest that multiple genetic variants within the autophagy
225 pathway have a cumulative influence and may further enhance the predictive power of

226 SNP analysis.

227 The putative function for each of the selected variants was predicted by the
228 SNPinfo program. We also used VEP
229 (http://asia.ensembl.org/info/docs/tools/vep/index.html) to predict the functions and
230 obtained similar results. Because the three SNPs identified in this study were tag
231 SNPs, there may be other variants in LD with the genotyped candidates as potentially
232 functional. Future studies are necessary to validate these SNPs in independent patient
233 populations. Additionally, fine mapping in the vicinity of these gene regions need to
234 be performed to identify potential causal variants.

235 We also further tested the rs2241880 variant in the A549 cell line. We found that
236 the effect of this variant was only observed in the migration assay. In the invasion
237 assay, differences were detected only between A549-300T and A549-Mock. The
238 T300A polymorphism only increased the migration ability of the cells. It is possible
239 that this effect of increasing the migration ability but not the invasion ability plays a
240 role in the development of BM.

241 Prophylactic radiotherapy has a clearly defined role in the treatment of patients
242 with high-risk acute lymphocytic leukemia. In SCLC, PCI has significantly improved
243 the overall survival rate in patients with either limited-stage disease (from 15% to
244 20% at 3 years) or extensive-stage disease (from 13% to 27% at 1 year) in patients
245 who respond to first-line treatment. Thus, PCI should be considered for the treatment
246 of all patients with extensive SCLC that responds to therapy and for patients with
247 limited-stage SCLC that responds to therapy. Even though the risk of brain failure in
248 NSCLC is not as high as that in SCLC, BM are quite common in NSCLC, with the
249 incidence ranging from 13% to 54%. [1] Thus, the use of PCI is also being considered
250 for NSCLC. PCI has consistently reduced or delayed the appearance of BM, but none

251 of the studies conducted to date has shown survival benefit. [7-9,11] According to Bovi
252 and White, [1] it is unclear whether this lack of survival benefit results from a failure to
253 identify the cohort best suited for preventive therapy; further, they imply that not all
254 patients with NSCLC should receive PCI. Moreover, the use of PCI to prevent
255 metastases can have both positive and negative effects. [40] Because no test can identify
256 which patients are at a high risk of developing BM, PCI has been administered
257 unselectively to all patients, which may result in unnecessary toxicity with little
258 potential benefit for some patients. Therefore, a validated nomogram should be
259 developed to predict the likelihood of BM in patients diagnosed with NSCLC. If the
260 findings from the current study are validated prospectively, in a study with adequate
261 statistical power, these results, in combination with clinicopathologic data, could
262 become the basis for selecting patient subgroups at a high risk of developing BM to
263 receive PCI.

264 In our study, the incidence of BM was 31% (101 of 323 patients), which is slightly
265 higher than in some studies. Clinicopathologic variables that may portend high risk of
266 BM include adenocarcinomatous histology, high-volume disease, and young age. [9]
267 Most of the patients in our study had adenocarcinoma histology, 45% had advanced
268 disease, and the median age (57 years) was lower than that typical for patients with
269 NSCLC. These differences may explain the relatively high incidence of BM in our
270 population; therefore, we adjusted for these variables in our multivariate analyses. We
271 further assessed whether the three genotypes were associated with metastasis risk at
272 other sites; no such association was detected. These results suggest that metastases in
273 the brain and elsewhere may arise through different mechanisms.

274 In our study, we only selected rs2241880 for our initial downstream functional
275 analysis, because the SNP in rs2241880 results in the substitution of threonine with

276 alanine, thereby changing the autophagy process. With regard to the other two SNPs,
277 *ATG10*: rs10036653 is near the 5′ end and *ATG12*: rs26532 is in the intron. Therefore,
278 we selected rs2241880 for our initial downstream functional analysis. The
279 downstream functions of the other two SNPs need to be analyzed in future studies.

280 In conclusion, to our knowledge, this study is the first to evaluate the associations
281 between genetic variations in the autophagy pathway and BM risk. We found that
282 three SNPs (*ATG16L1*: rs2241880, *ATG10*: rs10036653, and *ATG12*: rs26532) were
283 associated with BM risk. Because these results are based on the analysis of a
284 relatively small number of patients, we could not rule out the possibility of
285 false-positive findings. A further potential shortcoming is that we obtained
286 post-treatment computed tomography (CT) or magnetic resonance imaging (MRI)
287 scans only if clinical evaluation revealed suggestive findings such as neurological
288 symptoms. As is true in other studies analyzing the risk factors for BM, this could
289 limit the accuracy of a putative molecular marker of BM risk. Independent external
290 patient cohorts are needed to validate our findings. If validated, these SNPs may
291 prove to be valuable biomarkers for use in combination with clinicopathologic
292 variables to identify patients at high risk of BM who could benefit from PCI.

293 Materials and Methods

294 Study population and data collection

295 All patients in this retrospective analysis had histologically confirmed NSCLC that
296 had been treated at either the Tongji Hospital Cancer Center or the Hubei Provincial
297 Tumor Hospital in 2008–2011. No restrictions on age, gender, or disease stage were
298 applied, but all patients were required to have blood samples available for analysis.
299 The KPS of all patients was at least 70, and all had a life expectancy of at least 6
300 months. Epidemiologic data were collected with a structured questionnaire and

301 included information on demographics, smoking history, alcohol consumption,
302 medical history, family history of cancer, and occupational exposures to potential
303 carcinogens. Clinical and follow-up data on treatment regimens, disease stage,
304 pretreatment performance status, and vital status at the time of analysis were obtained
305 from the patients' medical records. CT or MRI scans had been obtained from each
306 patient before treatment as part of the disease staging process. All the patients were
307 asked to return to the hospital for examination (which included CT scans of the chest
308 and abdomen) every 2–3 months for the first 2–3 years after completion of treatment
309 and every 6 months thereafter. Repeat brain CT or MRI scans were obtained only in
310 the event of clinical indications such as neurological symptoms, as per the standard of
311 care. BM and survival information was collected from each patient's follow-up
312 records. Of the 363 patients eligible for this study, 40 were excluded, 16 because of
313 insufficient DNA for genotyping, 11 because of incomplete data on disease staging,
314 and 13 who had died or been lost to follow-up without information on BM, leaving
315 323 patients with complete information for the current analysis. Disease was staged
316 according to the tumor/nodes/metastasis system in the sixth (2002) edition of the
317 American Joint Committee on Cancer staging manual. Smoking status was coded as
318 current, former, or never smoked, as described previously. [41] The diagnosis of BM
319 was based on CT scans or MRI scans obtained as noted above. The time to BM was
320 defined as the interval from the date of NSCLC diagnosis to the date of BM diagnosis.
321 The follow-up time was the interval from NSCLC diagnosis to BM, death, or to the
322 last hospital visit.Patients with follow-up intervals longer than 24 months and those
323 without BM were censored at the date of the last contact. The study was approved by
324 the Ethics Committee of Tongji Medical College. Written informed consent was
325 obtained from all patients before interview.

326 **Polymorphism selection and genotyping**

327 Genomic DNA was isolated from peripheral blood lymphocytes by using a
328 QuickGene DNA whole blood kit S (Fujifilm, DB-S) according to the manufacturer's
329 protocol, and stored at –80 °C until use. Based on the public HapMap SNP database
330 and the HaploView 4.2 software, common SNPs (MAF ≥ 0.05) in six core genes of
331 autophagy (*ATG3*, *ATG5*, *ATG7*, *ATG10*, *ATG12*, and *LC3*) were screened in gene
332 regions (including the 10-kb upstream region of each gene) in the Chinese Han
333 population. After prediction with the SNPinfo Web Server (http://
334 snpinfo.niehs.nih.gov/), a total of 27 potentially functional SNPs were selected.
335 Linkage disequilibrium (LD) analysis with an r^2 threshold of 0.80 was further applied
336 to filter these functional SNPs. As a result, 16 loci were finally selected for genotyping.
337 However, rs2705507 was excluded because of design failure. Other SNPs previously
338 reported as being associated with survival or metastasis in general, were also included,
339 such as *ATG16L1*: rs2241880. A total of 16 SNPs were selected for genotyping (Table
340 4).

341 The SNPs were genotyped as described previously. [41]Sixteen of the SNPs were
342 genotyped by using MALDI-TOF mass spectrophotometry to detect allele-specific
343 primer extension products with the MassARRAY platform (Sequenom, Inc.). Assay
344 data were analyzed using the Sequenom TYPER software (version 4.0). The
345 individual call rate threshold was at least 95%.To assess reproducibility, 5% of the
346 DNA samples were blindly and randomly analyzed in duplicates, and the results
347 revealed a reproducibility of 99%.

348 **Cell lines and animals**

349 The A549 cell line, originating from human lung adenocarcinoma, was purchased
350 directly from ATCC prior to the described assays. Female BALB/c nu/nu mice (6

351 weeks old, Institute of Laboratory Animal Science) were bred in specific
352 pathogen-free conditions. Studies were conducted in compliance with the Chinese
353 guidelines for the care and use of laboratory animals and were approved by the
354 Institutional Animal Care and Use Committee of Tongji Medical College.

355 **Vector constructions**

356 First, we synthesized the ATG16L1 genetic template. In order to generate the entry
357 vectors, EF1α promoter, EGFP, or ATG16L1 was cloned into the genetic template, by
358 utilizing the Gateway® BP recombination reaction following the manufacturer's
359 instructions. To generate the entry vectors of ATG16L1 (mutation), the cDNAs were
360 first amplified by polymerase chain reaction with the generated template. The
361 resulting vectors, which we named pUp-EF1, pTail-IRES/eGFP, pDown-ATG16L1, or
362 pDown-ATG16L1 (mutation), were then recombined into the pDestpuro vector
363 generated following the protocol for LR recombination reaction using the Gateway®
364 LR plus clonase enzyme mix to construct expression lentiviral vectors, designated as
365 pLV(Exp)-Neo-EF1A> ATG16L1>IRES/EGFP and
366 pLV(Exp)-Neo-EF1A>ATG16L1(mutation)>IRES/EGFP.

367 The primers were as follows:

368 pD-ATG16L1(mutation)-PF1(59.8)

369 5′-GGGGACAAGTTTGTACAAAAAAGCAGGCTGCCACCATGTCGTCGGGCCT
370 CCG-3′

371 pD-ATG16L1(mutation)-PR1(63.2)

372 5′-GTAGCTGGTACCCTCACTTCTTTACCAGAACCAGGATGAGCATCCACATT
373 GTCCTGGGGGAC-3′

374 pD- ATG16L1(mutation)-PF2(63.6)

375 5′-GTCTCTTCCTTCCCAGTCCCCCAGGACAATGTGGATGCTCATCCTGGTTC

376 TGGTAAAGAAG-3′

377 pD-ATG16L1(mutation)-PR2(59.5)

378 5′-GGGGACCACTTTGTACAAGAAAGCTGGGTTCAGTACTGTGCCCACAGC-

379 3′

380 **In vitro assessment of ATG16L1 300T or ATG16L1 300A stable transfectants**

381 A549 cell lines stably expressing ATG16L1 (T300A) were generated by
382 lentivirus-mediated overexpression. The ATG16L1-300T or ATG16L1-300A cells
383 were transfected with an ATG16L1 (T300A)-overexpressing lentivirus at a
384 multiplicity of infection of 100 and then selected in media containing 2 μg/mL
385 puromycin(Invivogen, ant-pr-1). The transfection efficiency was measured in terms of
386 cellular expression of GFP by fluorescence microscopy (Leica DMI4000B). A549
387 cells stably transfected with ATG16L1 (T300A) were termed as A549-300T and
388 A549-300A. Transfectants receiving empty lentiviral vectors served as controls
389 (A549-Mock).

390 **Western blot analysis**

391 Cells were lysed in radioimmunoprecipitation assay (RIPA) buffer (Beyotime,
392 P0013B) supplemented with protease inhibitor (Beyotime, ST506). Protein
393 concentrations of the supernatant were determined using the BCA protein assay kit
394 (Beyotime, P0012S). Total protein (50 μg) was separated by SDS-PAGE and then
395 transferred onto a polyvinylidene fluoridemembrane (Millipore, IPVH00010). After
396 blocking with 5% BSA, the membranes were probed with the appropriate antibodies
397 (monoclonal rabbit anti-human ATG16L1 antibody (Cell Signaling Technology,
398 8089s) diluted at 1:1,000 and monoclonal mouse anti-human GAPDH antibody
399 (Beyotime, AF0006) diluted at 1:1,000. Horseradish peroxidase-conjugated goat
400 anti-rabbitIgG(Beyotime, A0208) and horseradish peroxidase-conjugated goat

401 anti-mouseIgG(Beyotime, A0216)diluted at 1:5,000 was used as the secondary
402 antibody. Proteins were detected with an enhanced SuperSignal West Pico
403 chemiluminescencekit(Pierce, 32109). GAPDH served as the internal standard. The
404 expression levels of GAPDH and ATG16L1 were quantified by using Image J.

405 **In vitro cell migration and invasion assays**

406 Transwell® migration assay

407 Cells (1×10^5) were suspended in 200 μL of Dulbecco's modified Eagle's medium
408 with 1% bovine serum albumin and seeded on the top chamber of the
409 Transwell®(Corning, 3422). Medium (900 μL) was added to the bottom chamber. The
410 cells were allowed to migrate for 12 h, and then stained with 0.1% crystal violet and
411 counted under a microscope.

412 Transwell® invasion assay

413 The Transwell® invasion assays (*in vitro* matrigel invasion assays) were performed
414 as described previously. [42] A549 cells(3×10^5) were suspended in200 μL of
415 Dulbecco's modified Eagle's medium with 1% bovine serum albumin, and were
416 added to the upper compartments of a 24-well Transwell® chamber containing
417 polycarbonate filters with 8-mm pores and coated with 60 mL of Matrigel (Sigma
418 Aldrich, E1270;1:9 dilution). Dulbecco's modified Eagle's medium (900 μL) with
419 10% bovine serum albumin was added to the lower chambers, and the chambers were
420 incubated for 24 h. Then, cells in the upper compartment were removed with a cotton
421 swab, rinsed with PBS (HyClone, SH30256.01B), and fixed in 100% methanol. Cells
422 that had invaded through the Matrigel to the lower surface were stained with
423 4,6-diamidino-2-phenylindole and quantified by counting the number of fluorescent
424 cells in five random microscopic fields per filter at 200× magnification.

425 **Metastasis assay via intracardiac inoculation**

The nude mouse model of brain metastasis via intracardiac inoculation was established as described previously.[43] Briefly, NSCLC cell lines were engineered to stably express a triple modality vector encoding GFP-luciferase fusion. Between 10^4 and 10^5 A549-300T, A549-300A, or A549-Mock cells were resuspended in 0.1 mL PBS (HyClone, SH30256.01B) and were injected into the right ventricle of nude mice (n = 8 per group). The animals were sacrificed 7 weeks later. Metastasis was detected by bioluminescence with an IVIS 200 Xenogen system and by histology. Incidence of brain metastasis was quantified on the basis of the presence of luminescent signal in the brain at 1,3,5, and 7 weeks after intracardiac inoculation.

Statistical analysis

Statistical analyses were performed with the SPSS software (version 16.0). A Cox proportional hazards model was used to calculate the HRs and 95% CIs to evaluate the influence of genotypes on BM risk. The model was adjusted for gender, age, disease stage, tumor histology, KPS, and smoking status. Kaplan–Meier curves were plotted to assess the cumulative BM probability. Log-rank tests were used to compare the differences between groups. All *P* values were two-sided, and *P* values <0.05 were considered statistically significant.

The *in-vitro* data were expressed as means ± SD from three independent experiments (each of which had been performed in triplicate) and were compared with Student’s t tests. *P* values of 0.05 were considered to indicate statistically significant differences.

Disclosure of Potential Conflicts of Interest

No potential conflicts of interest are disclosed.

Acknowledgments

We would like to thank Editage [www.editage.cn] for English language editing.

451 This study was funded by three grants from the National Natural Science
452 Foundation of China (grants 81472921, 81502521, and 81372664).

453 **References**

454 1. Bovi JA, White J. Radiation therapy in the prevention of brain metastases.
455 Curr Oncol Rep 2012; 14:55-62.

456 2. Subramanian A, Harris A, Piggott K, Shieff C, Bradford R. Metastasis to and
457 from the central nervous system--the 'relatively protected site'. Lancet Oncol
458 2002; 3:498-507.

459 3. Nathoo N, Chahlavi A, Barnett GH, Toms SA. Pathobiology of brain
460 metastases. J Clin Pathol 2005; 58:237-242.

461 4. Langer CJ, Mehta MP. Current management of brain metastases, with a focus
462 on systemic options. J Clin Oncol 2005; 23:6207-6219.

463 5. Nieder C, Bremnes RM, Andratschke NH. Prognostic scores in patients with
464 brain metastases from non-small cell lung cancer. J Thorac Oncol 2009;
465 4:1337-1341.

466 6. Cox JD, Stanley K, Petrovich Z, Paig C, Yesner R. Cranial irradiation in
467 cancer of the lung of all cell types. JAMA 1981; 245:469-472.

468 7. Russell AH, Pajak TE, Selim HM, Paradelo JC, Murray K, Bansal P, Cooper
469 JD, Silverman S, Clement JA. Prophylactic cranial irradiation for lung cancer
470 patients at high risk for development of cerebral metastasis: results of a
471 prospective randomized trial conducted by the Radiation Therapy Oncology
472 Group. Int J Radiat Oncol Biol Phys 1991; 21:637-643.

473 8. Umsawasdi T, Valdivieso M, Chen TT, Barkley HT, Jr., Booser DJ, Chiuten
474 DF, Dhingra HM, Murphy WK, Dixon CL, Farha P, et al. Role of elective
475 brain irradiation during combined chemoradiotherapy for limited disease

476 non-small cell lung cancer. J Neurooncol 1984; 2:253-259.
477 9. Gore EM, Bae K, Wong SJ, Sun A, Bonner JA, Schild SE, Gaspar LE, Bogart
478 JA, Werner-Wasik M, Choy H. Phase III comparison of prophylactic cranial
479 irradiation versus observation in patients with locally advanced non-small-cell
480 lung cancer: primary analysis of radiation therapy oncology group study
481 RTOG 0214. J Clin Oncol 2011; 29:272-278.
482 10. Li N, Zeng ZF, Wang SY, Ou W, Ye X, Li J, He XH, Zhang BB, Yang H, Sun
483 HB, et al. Randomized phase III trial of prophylactic cranial irradiation versus
484 observation in patients with fully resected stage IIIA-N2 nonsmall-cell lung
485 cancer and high risk of cerebral metastases after adjuvant chemotherapy. Ann
486 Oncol 2015; 26:504-509.
487 11. Cox JD, Scott CB, Byhardt RW, Emami B, Russell AH, Fu KK, Parliament
488 MB, Komaki R, Gaspar LE. Addition of chemotherapy to radiation therapy
489 alters failure patterns by cell type within non-small cell carcinoma of lung
490 (NSCCL): analysis of radiation therapy oncology group (RTOG) trials. Int J
491 Radiat Oncol Biol Phys 1999; 43:505-509.
492 12. Ceresoli GL, Reni M, Chiesa G, Carretta A, Schipani S, Passoni P, Bolognesi
493 A, Zannini P, Villa E. Brain metastases in locally advanced nonsmall cell lung
494 carcinoma after multimodality treatment: risk factors analysis. Cancer 2002;
495 95:605-612.
496 13. Robnett TJ, Machtay M, Stevenson JP, Algazy KM, Hahn SM. Factors
497 affecting the risk of brain metastases after definitive chemoradiation for
498 locally advanced non-small-cell lung carcinoma. J Clin Oncol 2001;
499 19:1344-1349.
500 14. Grinberg-Rashi H, Ofek E, Perelman M, Skarda J, Yaron P, Hajduch M,

501 Jacob-Hirsch J, Amariglio N, Krupsky M, Simansky DA, et al. The expression
502 of three genes in primary non-small cell lung cancer is associated with
503 metastatic spread to the brain. Clin Cancer Res 2009; 15:1755-1761.
504 15. Li Q, Yang J, Yu Q, Wu H, Liu B, Xiong H, Hu G, Zhao J, Yuan X, Liao Z.
505 Associations between single-nucleotide polymorphisms in the
506 PI3K-PTEN-AKT-mTOR pathway and increased risk of brain metastasis in
507 patients with non-small cell lung cancer. Clin Cancer Res 2013; 19:6252-6260.
508 16. Huang YH, Al-Aidaroos AQ, Yuen HF, Zhang SD, Shen HM, Rozycka E,
509 McCrudden CM, Tergaonkar V, Gupta A, Lin YB, et al. A role of autophagy in
510 PTP4A3-driven cancer progression. Autophagy 2014; 10:1787-1800.
511 17. Macintosh RL, Ryan KM. Autophagy in tumour cell death. Semin Cancer Biol
512 2013; 23:344-351.
513 18. Kenific CM, Thorburn A, Debnath J. Autophagy and metastasis: another
514 double-edged sword. Curr Opin Cell Biol 2010; 22:241-245.
515 19. Kondo Y, Kanzawa T, Sawaya R, Kondo S. The role of autophagy in cancer
516 development and response to therapy. Nat Rev Cancer 2005; 5:726-734.
517 20. Peng YF, Shi YH, Ding ZB, Ke AW, Gu CY, Hui B, Zhou J, Qiu SJ, Dai Z,
518 Fan J. Autophagy inhibition suppresses pulmonary metastasis of HCC in mice
519 via impairing anoikis resistance and colonization of HCC cells. Autophagy
520 2013; 9:2056-2068.
521 21. Zhu H, Wang D, Zhang L, Xie X, Wu Y, Liu Y, Shao G, Su Z. Upregulation of
522 autophagy by hypoxia-inducible factor-1alpha promotes EMT and metastatic
523 ability of CD133+ pancreatic cancer stem-like cells during intermittent
524 hypoxia. Oncol Rep 2014; 32:935-942.
525 22. Thiery JP, Acloque H, Huang RY, Nieto MA. Epithelial-mesenchymal

526 transitions in development and disease. Cell 2009; 139:871-890.
527 23. Tam WL, Weinberg RA. The epigenetics of epithelial-mesenchymal plasticity
528 in cancer. Nat Med 2013; 19:1438-1449.
529 24. Jo YK, Kim SC, Park IJ, Park SJ, Jin DH, Hong SW, Cho DH, Kim JC.
530 Increased expression of ATG10 in colorectal cancer is associated with
531 lymphovascular invasion and lymph node metastasis. PLoS One 2012;
532 7:e52705.
533 25. Desai SD, Reed RE, Babu S, Lorio EA. ISG15 deregulates autophagy in
534 genotoxin-treated ataxia telangiectasia cells. J Biol Chem 2013;
535 288:2388-2402.
536 26. Kim MS, Song SY, Lee JY, Yoo NJ, Lee SH. Expressional and mutational
537 analyses of ATG5 gene in prostate cancers. APMIS 2011; 119:802-807.
538 27. Huijbers A, Plantinga TS, Joosten LA, Aben KK, Gudmundsson J, den Heijer
539 M, Kiemeney LA, Netea MG, Hermus AR, Netea-Maier RT. The effect of the
540 ATG16L1 Thr300Ala polymorphism on susceptibility and outcome of patients
541 with epithelial cell-derived thyroid carcinoma. Endocr Relat Cancer 2012;
542 19:L15-18.
543 28. Zhao ZQ, Zheng HL, Zhu YG. Changes of plasma membrane AtPase activity,
544 membrane potential and transmembrane proton gradient in Kandelia candel
545 and Avicennia marina seedlings with various salinities. J Environ Sci (China)
546 2004; 16:742-745.
547 29. Cooney R, Baker J, Brain O, Danis B, Pichulik T, Allan P, Ferguson DJ,
548 Campbell BJ, Jewell D, Simmons A. NOD2 stimulation induces autophagy in
549 dendritic cells influencing bacterial handling and antigen presentation. Nat
550 Med 2010; 16:90-97.

551 30. Murthy A, Li Y, Peng I, Reichelt M, Katakam AK, Noubade R, Roose-Girma
552 M, DeVoss J, Diehl L, Graham RR, et al. A Crohn's disease variant in Atg16l1
553 enhances its degradation by caspase 3. Nature 2014; 506:456-462.
554 31. Salem M, Ammitzboell M, Nys K, Seidelin JB, Nielsen OH. ATG16L1: A
555 multifunctional susceptibility factor in Crohn disease. Autophagy 2015;
556 11:585-594.
557 32. Lassen KG, Kuballa P, Conway KL, Patel KK, Becker CE, Peloquin JM,
558 Villablanca EJ, Norman JM, Liu TC, Heath RJ, et al. Atg16L1 T300A variant
559 decreases selective autophagy resulting in altered cytokine signaling and
560 decreased antibacterial defense. Proc Natl Acad Sci U S A 2014;
561 111:7741-7746.
562 33. Saitoh T, Fujita N, Jang MH, Uematsu S, Yang BG, Satoh T, Omori H, Noda T,
563 Yamamoto N, Komatsu M, et al. Loss of the autophagy protein Atg16L1
564 enhances endotoxin-induced IL-1beta production. Nature 2008; 456:264-268.
565 34. Ohta K, Pang XP, Berg L, Hershman JM. Antitumor actions of cytokines on
566 new human papillary thyroid carcinoma cell lines. J Clin Endocrinol Metab
567 1996; 81:2607-2612.
568 35. Grimm WA, Messer JS, Murphy SF, Nero T, Lodolce JP, Weber CR, Logsdon
569 MF, Bartulis S, Sylvester BE, Springer A, et al. The Thr300Ala variant in
570 ATG16L1 is associated with improved survival in human colorectal cancer
571 and enhanced production of type I interferon. Gut 2016; 65:456-464.
572 36. Kongara S, Karantza V. The interplay between autophagy and ROS in
573 tumorigenesis. Front Oncol 2012; 2:171.
574 37. Oga A, Kong G, Ishii Y, Izumi H, Park CY, Sasaki K. Preferential loss of
575 5q14-21 in intestinal-type gastric cancer with DNA aneuploidy. Cytometry

576 2001; 46:57-62.
577 38. Ramus SJ, Pharoah PD, Harrington P, Pye C, Werness B, Bobrow L, Ayhan A,
578 Wells D, Fishman A, Gore M, et al. BRCA1/2 mutation status influences
579 somatic genetic progression in inherited and sporadic epithelial ovarian cancer
580 cases. Cancer Res 2003; 63:417-423.
581 39. Qin Z, Xue J, He Y, Ma H, Jin G, Chen J, Hu Z, Liu X, Shen H. Potentially
582 functional polymorphisms in ATG10 are associated with risk of breast cancer
583 in a Chinese population. Gene 2013; 527:491-495.
584 40. Sun A, Bae K, Gore EM, Movsas B, Wong SJ, Meyers CA, Bonner JA, Schild
585 SE, Gaspar LE, Bogart JA, et al. Phase III trial of prophylactic cranial
586 irradiation compared with observation in patients with locally advanced
587 non-small-cell lung cancer: neurocognitive and quality-of-life analysis. J Clin
588 Oncol 2011; 29:279-286.
589 41. Li Q, Wu H, Chen B, Hu G, Huang L, Qin K, Chen Y, Yuan X, Liao Z. SNPs
590 in the TGF-beta signaling pathway are associated with increased risk of brain
591 metastasis in patients with non-small-cell lung cancer. PLoS One 2012;
592 7:e51713.
593 42. Yuan X, Wei Q, Komaki R, Liu Z, Yang J, Tucker SL, Xu T, Heymach JV, Lu
594 C, Cox JD, et al. Polymorphisms Predict Distant Metastasis-Free Survival in
595 Patients with Inoperable Non-Small-Cell Lung Cancer after Definitive
596 Radiotherapy. PLoS One 2013; 8:e65659.
597 43. Nguyen DX, Chiang AC, Zhang XH, Kim JY, Kris MG, Ladanyi M, Gerald
598 WL, Massague J. WNT/TCF signaling through LEF1 and HOXB9 mediates
599 lung adenocarcinoma metastasis. Cell 2009; 138:51-62.

600 **FIGURE LEGENDS**

601 **Figure 1**. Kaplan-Meier estimates of the cumulative probability of brain metastasis
602 among patients with non-small cell lung cancer according to the following genotypes:
603 (A) *ATG10*: rs10036653; (B) *ATG16L1*: rs2241880; (C) *ATG12*: rs26532; and (D)
604 combined. The AA genotype at rs10036653, the AA genotype at rs2241880, and the
605 AC/CC genotype at rs26532 were associated with higher cumulative probability of
606 brain metastasis than the other genotypes.
607 **Figure 2**. Transfection of A549 lung cancer cell line with lentivirus for ATG16L1
608 rs2241880 300T or 300A. (A) pLV(Exp)-Neo-EF1A>ATG16L1>IRES/EGFP and
609 pLV(Exp)-Neo-EF1A>ATG16L1(mutation)>IRES/EGFP system. (B) Fluorescence
610 labeling indicated that the transfection efficiency was 99% for both cell lines. (C)
611 Western blot analysis confirmed that transfection with either 300T or 300A led to
612 overexpression of ATG16L1. A549-Mock (transfectants that received empty lentiviral
613 vectors) served as controls. Glyceraldehyde-3-phosphate dehydrogenase (GADPH)
614 was used as a loading control.
615 **Figure 3**. Effect of transfection with rs2241880 T300A on the migration and invasion
616 of A549 cells. (A) In the Transwell® migration assays, the 300T transfectants showed
617 greater migration than the 300A transfectants. (B) In the Transwell® invasion assays,
618 the 300T transfectants showed greater invasiveness than the A549-Mock cells. *$P <$
619 0.05, **$P < 0.01$. Results are presented as means from three independent experiments;
620 error bars represent standard deviation.
621 **Figure 4**. *In vivo* analysis of the effect of transfection with rs2241880 T300A on
622 metastasis. (A) Metastasis was detected by measuring the bioluminescence with an
623 IVIS 200 Xenogen system. (B) Percentage of brain metastasis: 42.9% in the
624 A549-300T group, 14.2% in the A549-300A group, and 12.5% in the A549-Mock
625 group, respectively. (C) Three-dimensional imaging of brain metastases. (D)

626 Metastasis was detected by histology; brain metastasis (100×) and brain metastasis
627 (200×).

Table 1. Patient- and disease-related characteristics and their association with brain metastasis

Characteristic	No. of Patients (%)	No. of Events (%)	Univariate Analysis			Multivariate Analysis		
			HR	(95% CI)	*P* Value	HR	(95% CI)	*P* Value
Sex								
Female	102 (32)	30 (29)	1.000			1.000		
Male	221 (68)	71 (32)	1.105	0.721-1.693	0.646	0.972	0.571-1.655	0.918
Age, years								
≥ 60 years	132(41)	37 (28)	1.000			1.000		
< 60 years	191(59)	64 (34)	1.253	0.836-1.879	0.275	1.056	0.696-1.603	0.796
Median (range)	58 (26-82)							
Disease stage at diagnosis								
I, II, IIIA	177 (55)	38 (22)	1.000			1.000		
IIIB, IV	146 (45)	63 (43)	2.520	1.683-3.772	<0.001	2.517	1.657-3.823	<0.001
Tumor histology								
Squamous cell	80 (25)	19 (24)	1.000			1.000		
Adenocarcinoma	223 (69)	78 (35)	1.567	0.949-2.588	0.079	1.419	0.827-2.435	0.204
NSCLC, NOS	20 (6)	4 (20)	0.816	0.278-2.400	0.712	0.764	0.256-2.280	0.630
KPS Score								
>80	39 (12)	11 (28)	1.000			1.000		
80	210 (65)	63 (30)	1.073	0.565-2.035	0.830	0.731	0.373-1.433	0.362
<80	74 (23)	27 (37)	1.371	0.680-2.763	0.378	1.059	0.516-2.173	0.876
Tobacco Smoking Status								
Current	131 (40)	45 (34)	1.000			1.000		
Former	35 (11)	13 (37)	1.123	0.606-2.082	0.713	0.931	0.495-1.751	0.825
Never	157 (49)	43 (27)	0.781	0.514-1.186	0.246	0.677	0.401-1.145	0.146

Multivariate analyses were adjusted for all of the factors listed in this table.

Table 2. Associations between genotypes and brain metastases

Characteristic	No. of	No. of	Univariate Analysis			Multivariate Analysis*		
	Patients	Events(%)	HR	(95% CI)	*P* Value	HR	(95% CI)	*P* Value
ATG10: rs10036653								
AA	116	45(39)	1.000			1.000		
AT + TT	192	55(29)	0.692	0.467–1.026	0.067	0.596	0.398–0.894	0.012
ATG16L1: rs2241880								
AA	131	51(39)	1.000			1.000		
AG + GG	186	49(26)	0.617	0.416–0.913	0.016	0.655	0.438–0.978	0.039
ATG12: rs26532								
AA	117	26 (22)	1.000			1.000		
AC + CC	200	73 (37)	1.718	1.098–2.689	0.018	1.644	1.049–2.576	0.030

*NOTE. Multivariate analyses in this table were adjusted for sex, patient age, tumor histology, disease stage, Karnofsky Performance Status, and smoking status.

Abbreviations: HR, hazard ratio; CI, confidence interval; BM, brain metastases.

Table 3. Associations between genotypes and brain metastases

Characteristic	No. of	No. of	Univariate Analysis			Multivariate Analysis*		
	Patients	Events(%)	HR	(95% CI)	*P* Value	HR	(95% CI)	*P* Value
0	65	11 (17)	1.000			1.000		
1	170	53 (31)	1.992	1.041–3.814	0.038	1.942	1.010–3.735	0.047
2	78	35(45)	3.077	1.562–6.061	0.001	3.051	1.543–6.033	0.001

*NOTE. Multivariate analyses in this table were adjusted for sex, patient age, tumor histology, disease stage, Karnofsky Performance Status, and smoking status.

Abbreviations: HR, hazard ratio; CI, confidence interval; BM, brain metastases.

Table 4. Genes and single nucleotide polymorphisms selected for analysis

Gene (number of SNPs)	SNP	Allelic change	SNP Position	TFBS	Splicing (ESE or ESS)	nsSNP	Polyphen	Impact
ATG3(1)	rs7652377	C > A	intron	Y	-	-	-	modifier
ATG5(3)	rs510432	G > A	near 5′	Y	-	-	-	modifier
	rs688810	T > C	intergenic	Y	-	-	-	modifier
	rs3804338	C > T	intron	Y	-	-	-	modifier
ATG7(3)	rs8154	T > C	synon	-	Y	-	-	modifier
	rs1375206	C > G	intron	Y	-	-	-	modifier
	rs1470612	G > A	intron	Y	-	-	-	modifier
ATG10(5)	rs1864183	A> G	missense	-	Y	Y	possiblydamaging	moderate
	rs1864182	T > G	missense	-	Y	Y	benign	moderate
	rs10514231	T > C	intron	Y	-	-	-	modifier
	rs10036653	A > T	near 5′	Y	-	-	-	modifier
	rs3734114	T > C	missense	-	Y	Y	benign	moderate
ATG12(3)	rs26532	A > C	intron	Y	-	-	-	modifier
	rs26534	G > A	near 5′	Y	-	-	-	modifier
	rs26538	C > T	intron	Y	-	-	-	modifier
ATG16L1(1)	rs2241880	T > C	missense	-	Y	Y	benign	moderate

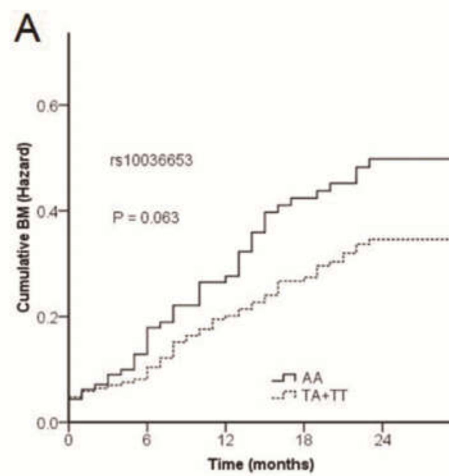
A
rs10036653
P = 0.063
AA
TA+TT
Cumulative BM (Hazard)
0.0
0.2
0.4
0.6
0
6
12
18
24
Time (months)

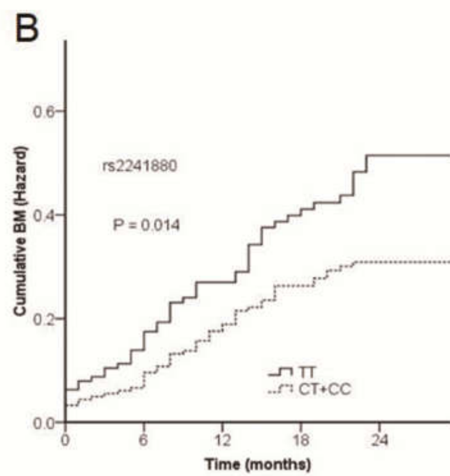
B
rs2241880
P = 0.014
TT
CT+CC
Cumulative BM (Hazard)
0.0
0.2
0.4
0.6
0
6
12
18
24
Time (months)

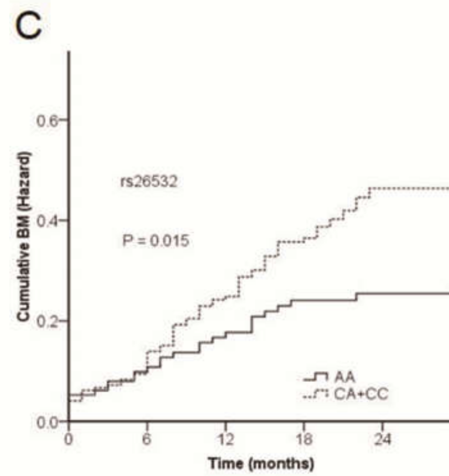
C
rs26532
P = 0.015
AA
CA+CC
Cumulative BM (Hazard)
0.0
0.2
0.4
0.6
0
6
12
18
24
Time (months)

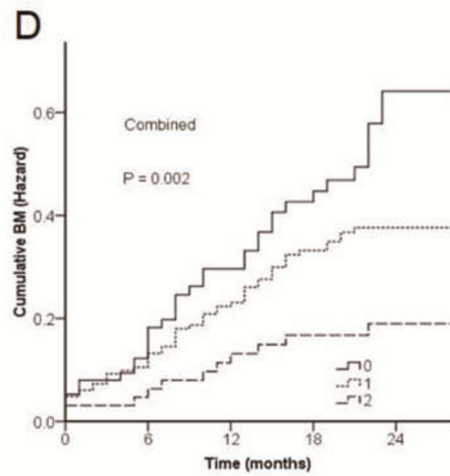
D
Combined
P = 0.002
0
1
2
Cumulative BM (Hazard)
0.0
0.2
0.4
0.6
0
6
12
18
24
Time (months)

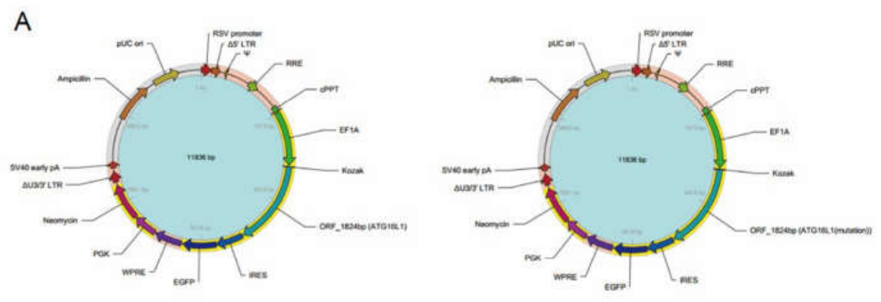
A
pUC ori
RSV promoter
Δ5' LTR
Ψ
RRE
cPPT
EF1A
Kozak
ORF_1824bp (ATG16L1)
IRES
EGFP
WPRE
PGK
Neomycin
ΔU3/3' LTR
SV40 early pA
Ampicillin
11836 bp
ORF_1824bp (ATG16L1(mutation))

B
A549-Mock
A549-300T
A549-300A
200um
200um
200um

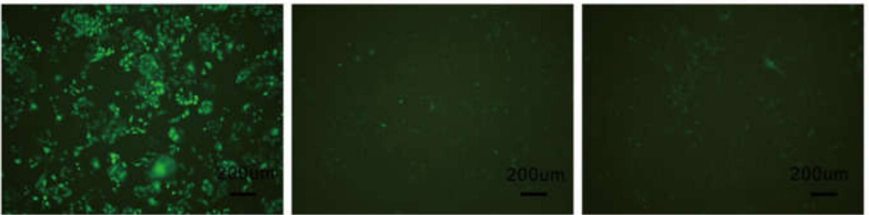
200um
200um
200um

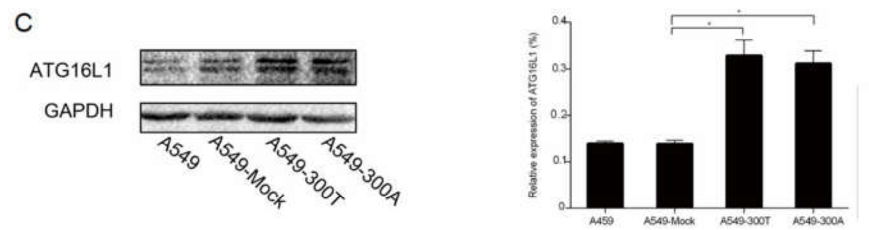
C
ATG16L1
GAPDH
A549
A549-Mock
A549-300T
A549-300A
Relative expression of ATG16L1 (%)
0
0.1
0.2
0.3
0.4
*
*
A459
A549-Mock
A549-300T
A549-300A

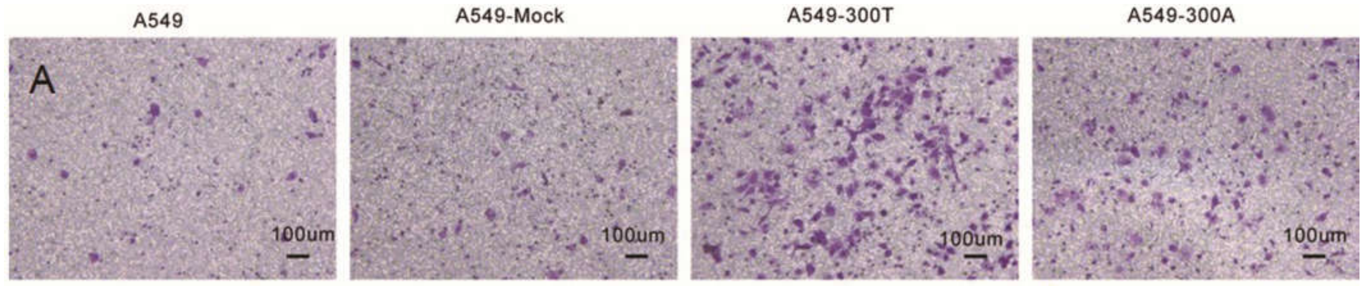
A549
A549-Mock
A549-300T
A549-300A
A
100um
100um
100um
100um
Number of migration cells
150
100
50
0
**
**
**
A459
A549-Mock
A549-300T
A549-300A
Number of invasion cells
250
200
150
100
50
0
**
A549
A549-Mock
A549-300T
A549-300A

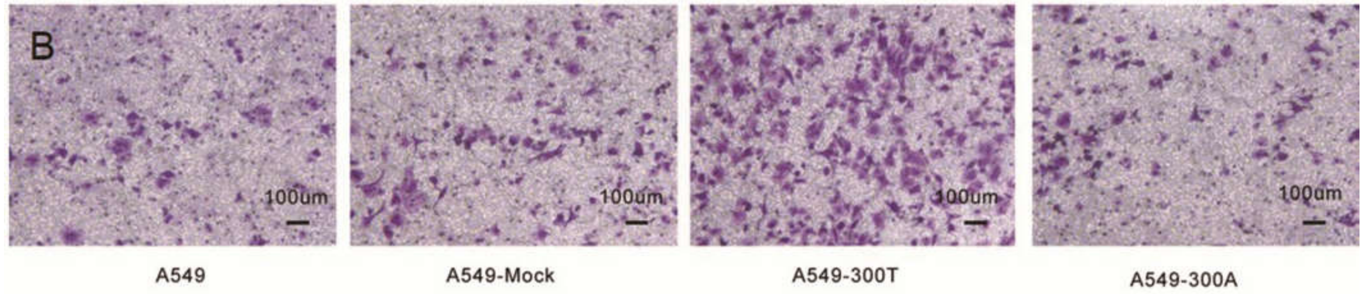
B
100um
100um
100um
100um
A549
A549-Mock
A549-300T
A549-300A

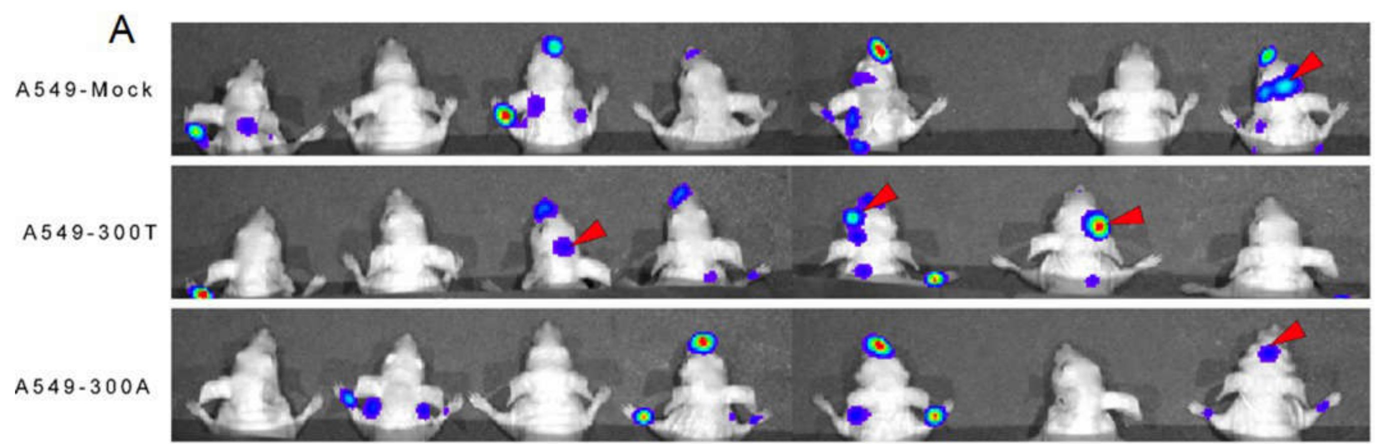
A
A549-Mock
A549-300T
A549-300A

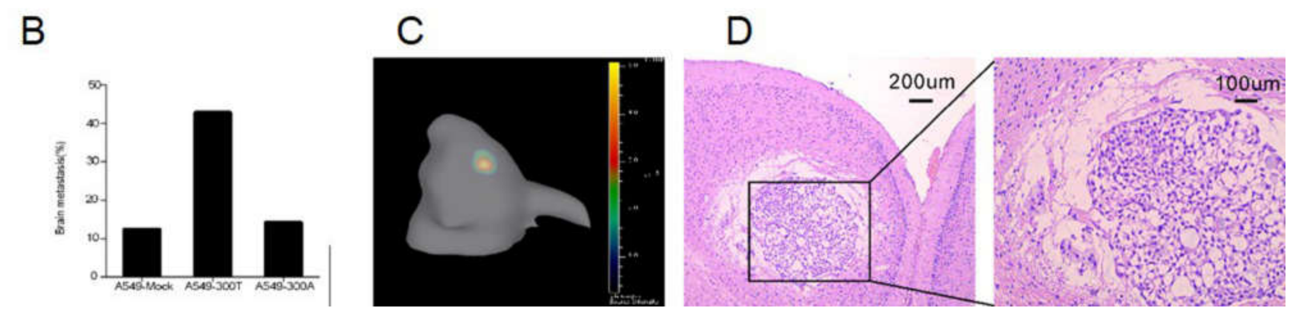
B
Brain metastasis(%)
0
10
20
30
40
50
A549-Mock
A549-300T
A549-300A
C
D
200um
100um